Drosophila p38 MAPK Interacts with BAG-3/starvin to Regulate Age-dependent Protein Homeostasis

Sarah M. Ryan[2,*], Michael Almassey[1,*], Amelia M. Burch[3], Gia Ngo[2], Scott Barbee[2], Nathan T. Mortimer[1], Subhabrata Sanyal[3,4] and Alysia D. Vrailas-Mortimer[1-3]

1 Illinois State University, School of Biological Sciences, Normal, IL, USA

2 University of Denver, Department of Biological Sciences, Denver, CO, USA

3 Emory University, Department of Cell Biology, Atlanta, GA, USA

4 Calico, San Francisco, CA, USA

Running Title: p38K Regulates Age-Dependent Proteostasis

Key words/phrases: p38 MAPK, BAG-3/starvin, protein aggregation, aging, Lamin

Corresponding author:
Alysia D. Vrailas-Mortimer
Illinois State University
School of Biological Sciences
Science Laboratory Building
Normal, IL 61790
Phone: 309-348-8574
Fax: 309-348-3722
e-mail: admorti@ilstu.edu

Summary

As organisms age, they often accumulate protein aggregates that are thought to be toxic, potentially leading to age-related diseases. This accumulation of protein aggregates is partially attributed to a failure to maintain protein homeostasis. A variety of genetic factors have been linked to longevity, but how these factors also contribute to protein homeostasis is not completely understood. In order to understand the relationship between aging and protein aggregation, we tested how a gene that regulates lifespan and age-dependent locomotor behaviors, p38 MAPK (p38Kb), influences protein homeostasis as an organism ages. We find that p38Kb regulates age-dependent protein aggregation through an interaction with the Chaperone-Assisted Selective Autophagy complex. Furthermore, we have identified Lamin as an age-dependent target of p38Kb and the Chaperone-Assisted Selective Autophagy complex.

Introduction

Protein turnover is critical for maintaining tissue health as many proteins become damaged or misfolded during normal tissue functions. Therefore, the cell utilizes a variety of protein quality control mechanisms to refold or degrade these damaged proteins, including the ubiquitin proteasome system and macroautophagy. During aging, protein quality control mechanisms become less efficient leading to the accumulation of damaged or misfolded proteins that begin to form protein aggregates[1]. It has been hypothesized that these aggregates are toxic and may lead to the deleterious phenotypes associated with normal aging, such as impaired tissue function[1]. Furthermore, decreased protein aggregation has been associated with longevity. For example, over-expression of Foxo leads to an increased lifespan but also a concordant

decrease in protein aggregation in *C. elegans*, *Drosophila,* and mice [2–6], suggesting that lifespan and protein aggregation are tightly linked processes. However, the molecular mechanisms that underlie the relationship between aging and protein homeostasis have not been fully characterized.

One pathway that has been linked to both aging and protein homeostasis is the stress response p38 MAPK (p38K) pathway. In mammals, there are four p38K genes (α, β, γ, and δ), and p38Kα has been linked to both the inhibition [7,8] and induction [9,10] of macroautophagy, in particular in response to oxidative stress [11,12]. In addition, p38Kα has been linked to regulating macroautophagy in cellular senescence [13–15]. However, how p38K signaling may contribute to protein homeostasis in response to natural aging is not well understood. The fruit fly *Drosophila melanogaster* has two canonical p38K genes (p38Ka and p38Kb), and we have previously reported that p38Kb acts in the adult musculature to regulate aging. We found that over-expression of p38Kb leads to increased lifespan while loss of p38Kb results in a short lifespan and age-dependent locomotor behavior defects [16]. In addition, oxidatively damaged proteins accumulate in the muscle of p38Kb mutants with age [16], and loss of p38Kb leads to increased polyubiquitination of insoluble proteins and alterations in oxidative stress dependent translation [17], suggesting that these oxidatively damaged proteins may be aggregating in p38Kb mutants. Furthermore, p38Kb has been shown in a *Drosophila* cell culture system to pull down with the HspB8 homologue CG14207 [18], which plays a role in the muscle by regulating protein homeostasis as a part of a protein quality control mechanism called BAG-3 Mediated Selective Autophagy pathway or the Chaperone-Assisted Selective Autophagy (CASA) complex in flies [19,20]. The CASA complex also includes the chaperone Hsc70 and the co-chaperone BAG-3 (starvin in flies). BAG-3/starvin binds to specific damaged or misfolded protein substrates and brings them to the CASA complex

where it binds to Hsc70 and HspB8. Those substrates that cannot be refolded by the complex are polyubiquitinated and targeted to the autophagosome through a handover between BAG-3/stv and the autophagy adaptor protein p62 (ref(2)p in flies), and subsequently degraded through the autophagosome-lysosome system [21–25].

Here, we report that p38Kb regulates age-dependent muscle protein homeostasis through an interaction with the CASA complex. We find that p38Kb acts as an intermediary between BAG-3/starvin and p62/ref(2)p in targeting damaged or misfolded proteins for degradation. This interaction is not only important for maintaining protein homeostasis but also for lifespan extension. In addition, we find that the *Drosophila* homologue of the Hutchinson-Gilford progeria protein, Lamin A/C, is a target for p38Kb and CASA complex mediated protein turnover, suggesting that the p38Kb aging phenotypes may be a result of impaired Lamin degradation.

Materials and Methods

Genotypes

UAS-p38Kb wt, UAS-p38Kb Kinase Dead, p38Kb$^{\Delta 45}$, p38Kb^{Ex41}, w^{1118}, Mef2-GAL4 and MHC-GAL4 were as described in [16]. The p38Kb^{Ex41} is a precise excision allele and serves as a genetic background control for p38Kb$^{\Delta 45}$ deletion mutation.

UAS-stv RNAi 34408 (w^{1118}; P{GD10796}v34408) and UAS-stv RNAi 34409 (w^{1118}; P{GD10796}v34409/TM3) are described in [26] and are from the Vienna Drosophila Resource Center.

stv-GFP trap (w^{11118};; Pbac{754.P.F3v30} $stv^{+CPTI\ 002824}$), HspB8-GFP trap (w^{1118} PBac{810.P.FSVS-2}$CG14207^{CPTI004445}$), Hsc70-4 GFP trap (*w^{1118} PBac{544.SVS-1}$N^{CPTI002347}$*) are from the Kyoto Stock Center.

w^{1118}; P{y[+mDint2] w[BR.E.BR]=SUPor-P}ref(2)$P^{KG00926}$, w^{1118};;+mDint2 EY4969 stvEP, Lam^{A25} pr^{1}, and w^{1118}; P{w[+mC]=UAS-Lam.GFP}3-3 were obtained from the Bloomington Drosophila Stock Center.

All fly stocks were backcrossed into the w^{1118} background and isogenized for 10 generations. All stocks were reared at 25ºC in a 12hr:12hr light:dark cycle on standard fly food media.

Immunofluorescence

Adult flies were fixed in 4% paraformaldehyde for 48hrs at 4°C. Indirect flight muscles were dissected in 1X PBS, permeabilized in 1X PBS 0.15% Triton-X 100, and blocked in NGS + 0.15% Triton-X 100. Samples were incubated in primary antibody at 4°C overnight, washed in 1X PBS 0.15% Triton-X 100, and incubated in secondary antibody at room temperature for 2hrs. Samples were mounted in Vectashield mounting medium (Vectorlabs) and visualized using a laser scanning confocal microscope. Antibodies: rabbit anti-GFP 1:400 (Invitrogen), mouse anti-FLAG M2 1:1000 (Sigma), rabbit anti-stv 1:1000 (gift of Jrög Höhfeld), rat anti-α actinin 1:100 (Abcam), rabbit anti-ubiquitin linkage-specific K63 anti-mouse 1:200 (Abcam), IgG- Alexa Fluor 488 1:200 (Life Technologies), anti-mouse IgG- Alexa Fluor 568 1:500 (Life Technologies), anti-rabbit IgG- Alexa Fluor 488 1:500 (Life Technologies) and Rhodamine Phalloidin 1:2000.

Protein aggregate analysis

Indirect flight muscles were prepared as described above from 9 individual flies per genotype. Protein aggregates were identified using mouse anti-polyubiquitin 1:1000 (Enzo Life Sciences). Three muscles from each individual fly were imaged as z-series and flattened into a single image as a max projection using confocal microscopy for a total of 27 muscles per genotype. Images were analyzed using Image J "Analyze Particles" function with a diameter of 100 pixels set for the minimum aggregate size. Aggregate number and size were analyzed using ANOVA followed by Tukey's HSD using the R package "multcomp" to generate significance groups with each letter group being significantly different with a p value of ≤ 0.05. Within genotype/across time point analyses were performed using the Welch two sample t-test in R.

Lifespan

For lifespan experiments using the UAS-p38Kb^{wt}, ref(2)p -/+, p38Kb$^{\Delta 45/\Delta 45}$, the stv EP (stv^{wt}) lines, and their respective controls, virgin females were kept on standard molasses *Drosophila* media. Due to a change in lab food, the stv RNAi 34408 and stv RNAi 34409 lifespan experiments (with their respective controls) were performed on the standard Bloomington *Drosophila* media. Virgin flies were collected and reared at 25°C in a 12hour:12hour light:dark cycle. Flies were put on new food twice a week. The number of dead animals was scored daily. Lifespan was analyzed using a log rank test to compare genotypes with censored data on all genotypes and then on all pairwise comparisons using the R package "survival" with Benjamini and Hochberg correction (false discovery rate < 0.05).

Co-immunoprecipitation

Flies were aged 1 week or 5 weeks. Forty thoraxes per genotype per condition were homogenized in high salt buffer (0.5 M KCl, 35% glycerol,10 mM HEPES pH 7.0, 5 mM

183 $MgCl_2$, 0.5 mM EDTA pH 8.0, 0.1% NP40 25 mM NaF, 1 mM Na_2VO_4, 1 mM DTT,
184 Complete protease inhibitor). The lysate was flash frozen in liquid nitrogen and quickly
185 thawed at 37°C. Then lysates were rocked at 4°C for 30 minutes and centrifuged at
186 14,200 x g for 30 minutes at 4°C. The supernatant was transferred to equilibrated beads
187 anti-Flag (M2) agarose (Sigma) or anti-GFP agarose (Chromotek) and rocked for 2
188 hours at 4°C. Beads were collected using a magnetic bar and washed four times with IP
189 buffer (50 mM HEPES pH 7.0, 100 mM KCl, 0.4% NP40 1.5 mM $MgCl_2$, 5% glycerol, 25
190 mM Na, 1 mM Na_2VO_4, 1 mM EDTA, 1 mM DTT, Complete protease inhibitor). Lysates
191 were then analyzed by immunoblotting using rabbit anti- GFP 1:1000 (Invitrogen),
192 mouse anti-FLAG M2 1:1000 (Sigma), rabbit anti-phospho-p38 1:1000 (Cell Signaling
193 Technologies), goat anti total p38 1:1000 (Santa Cruz Biotechnology), rabbit anti-stv
194 1:10,000 (gift of Jrög Höhfeld) or mouse anti-Lamin 1:1000 (DHSB).
195
196 **Immunoblotting**
197 Wild type flies (w^{1118}) were aged either for 3, 15, 30, and 45 days or for 1-5 weeks. Three
198 thoraxes were dissected and homogenized in 1x Laemmli buffer. Immunoblots were
199 performed as described in [16]. Membranes were developed using SuperSignal West
200 Femto kit (ThermoFisher) or Pierce ECL (ThermoFisher) and exposed on
201 autoradiography film. Antibodies used were: rabbit anti-GFP 1:1000 (Invitrogen), rabbit
202 anti-starvin 1:10,000 (gift of Jrög Höhfeld), mouse anti-actin 1:5,000,000 (Sigma), mouse
203 anti-FLAG M2 (Sigma), rabbit anti-alpha tubulin (Cell Signaling Technologies), mouse
204 anti-Lamin 1:100 (DHSB), rabbit anti-phospho Lamin A Ser22 1:1000 (Thermofisher),
205 mouse anti-beta tubulin (E-10) 1:5000 (Santa Cruz Biotechnology), mouse anti- HRP
206 1:20,000 (Jackson Labs), rabbit anti-HRP 1:40,000 (Jackson Labs). Densitometry was
207 performed using a minimum of three independent blots. For statistical analysis of protein

208 expression level, pixel density of the tested protein was normalized within sample to the
209 loading control. These values were then normalized to control to calculate fold change.
210 The fold change values were analyzed by Student's t-test or ANOVA [27] as appropriate.
211
212 **Sucrose Gradient Fractionation**
213 p38Kb$^{Ex41/Ex41}$ and p38Kb$^{\Delta45/\Delta45}$ flies were aged three weeks. 30 thoraxes per genotype
214 were dissected and homogenized in NP40 lysis buffer. Samples were centrifuged at
215 800xg for 10 minutes at 4°C. The supernatant was then transferred to a 15-50% sucrose
216 discontinuous gradient. Samples were then ultracentrifuged at 55,000 rpm (201,000xg at
217 r_{av}) for 20 hours at 4°C in a TLS-55 in a Beckman Coulter Optima TLX Ultracentrifuge.
218 200µl fractions were collected and the pellet was resuspended in an equal volume of
219 NP40 Lysis Buffer.
220
221 **Stv localization**
222 Immunohistochemistry on p38Kb$^{Ex41/ Ex41}$ and p38Kb$^{\Delta45/\Delta45}$ Indirect flight muscles was
223 performed as described above. Confocal images from five individual flies per genoytpe
224 were analyzed for average pixel density using ImageJ in three different non-overlapping
225 locations on each muscle for a total of 15 measurements per genotype. Average pixel
226 density was analyzed by Student's t-test using R.
227
228 **Results**
229
230 **p38Kb regulates age-dependent protein homeostasis.**
231 p38Kb null mutant animals (p38Kb$^{\Delta45/\Delta45}$, a deletion of the p38Kb gene) exhibit age-
232 dependent locomotor behavior defects and have a 48% lifespan reduction. In addition,

biochemical analysis suggests that p38Kb null mutants have increased levels of insoluble polyubiquitinated proteins in the thoracic musculature of aged animals as observed by immunoblot analysis [17]. However, protein aggregate size and distribution have not been visualized in the p38Kb mutants, nor is it known whether augmenting p38Kb activity in muscles leads to a change in protein homeostasis. Therefore, we analyzed how p38Kb expression influences protein aggregation. We find that p38Kb null mutants have an increased number of protein aggregates in the adult indirect flight muscle at 1 week and 3 weeks of age (Figure 1A-B and E-F, Table S1) and increased aggregate size with age (Figure 1G-H, Table S1) as compared to a genetic background control ($p38Kb^{Ex41/Ex41}$, a precise excision allele). Furthermore, transgenic inhibition of p38Kb in the muscle using a dominant negative kinase dead construct ($p38Kb^{KD}$, [16]) also results in a significant increase in aggregate number, however aggregate size was not affected (Figure 1I-L and Table S2). Conversely, as both strong and moderate levels of p38Kb over-expression lead to an increased lifespan (37% and 14% extension, respectively) [16], we tested if p38Kb over-expression also affects protein aggregation. We find that both strong over-expression of p38Kb in the adult muscle using the Mef2-GAL4 driver (Figure 1C-D and M-P, Table S3) and moderate over-expression of p38Kb using the MHC-GAL4 driver (Figure 1Q-T and Table S4) leads to decreased protein aggregate number and size throughout the lifespan. It has been hypothesized that protein aggregate accumulation and increased size may be toxic, potentially explaining the decreased lifespan and age-dependent locomotor abnormalities in $p38Kb^{\Delta 45}$ null mutants and the increased longevity in the p38Kb over-expression animals.

p38Kb mediates age-dependent phenotypes through autophagy

In order to determine what mechanism plays a role in the clearance of polyubiquitinated protein aggregates, we first tested what type of ubiquitin linkage is present in the

aggregates in wild type flies. In particular, K63-linked ubiquitination has been shown to facilitate the formation of aggregates [28–30] that are cleared through autophagy [30–32]. We find that a subset of aggregates from aging flies contain K63-linked ubiquitinated proteins (Figure 2A-C), suggesting that these muscle protein aggregates are degraded through autophagy. Polyubiquitinated protein aggregates can be degraded through selective autophagy in which the adaptor protein p62 (ref(2)p in flies) promotes the packaging and delivery of polyubiquitinated proteins to the autophagosome [33]. If p38Kb requires selective autophagy to mediate protein homeostasis, then loss of ref(2)p will block the p38Kb mediated decreased aggregation phenotype. We find that loss of a single copy of *ref(2)p* results in fewer aggregates (Figure 2D-E and Table S5), which may reflect compensation by other protein clearance mechanisms with aging, especially as homozygous *ref(2)p* mutants are viable. When a single copy of *ref(2)p* is removed in the p38Kb over-expression background, this prevents the reduced protein aggregation observed in the p38Kb over-expression animals at both young and old ages (Figure 2D-E and Table S5). This dominant interaction suggests that *ref(2)p* acts downstream of p38Kb to promote the degradation of protein aggregates.

p38Kb colocalizes with the CASA complex in the adult flight muscle.

In order to better understand the role of p38Kb in protein homeostasis, we first determined where in the muscle p38Kb localizes and find that a FLAG-tagged p38Kb (green) colocalizes with the Z-disc marker alpha-actinin and is also present at the M-line (Figure 2F). The muscle Z-disc is an area of high protein turnover, and one protein quality control mechanism that localizes to the Z-disc in mice and adult flies is the Chaperone-Assisted Selective Autophagy (CASA) complex [19,34]. In adult *Drosophila* muscle, the CASA complex has been reported to consist of the Hsc70 homologue, Hsc70-4, the HspB8 homologue CG14207 and the BAG-3 homologue starvin (stv) [19].

We find that p38Kb colocalizes with all the CASA complex members at the Z-disc and M-line (Figure 2G-I).

p38Kb physically interacts with the CASA complex in the adult flight muscle.

In order to further determine if p38Kb physically interacts with the CASA complex in the adult muscle, we performed co-immunoprecipitation experiments. In *Drosophila* cell culture $p38Kb^{wt}$ was shown to co-immunoprecipitate with the HspB8 homologue CG14207[18], therefore, we tested if this interaction also occurs in adult indirect flight muscle. As the interaction between p38Kb and its targets may be transient, we utilized a FLAG-tagged p38Kb kinase dead construct (UAS-$p38Kb^{KD}$ Mef2-GAL4) that is able to be activated and bind to a target but cannot phosphorylate it, leading to a delayed release of the target[35]. We expressed $p38Kb^{KD}$ in the adult flight muscle of a fly that also endogenously expressed GFP tagged HspB8, in which GFP is spliced in as a new exon of the endogenous gene. This results in a GFP fusion protein that is expressed in the same pattern as endogenous HspB8 ([19] and Figure 2H'). We find that $p38Kb^{KD}$ was able to pull down HspB8 (Figure 2J) as compared to the HspB8-GFP control background. In addition, expression of $p38Kb^{KD}$ in a wildtype background was able to pull down un-tagged endogenous stv (Figure 2K). We then performed reverse IPs in which we immunoprecipitated each endogenously GFP tagged CASA complex protein (Hsc70-4, HspB8, or stv) and probed for FLAG tagged $p38Kb^{KD}$ and found that p38Kb co-immunoprecipitates with the CASA complex (Figure 2L-N) with stronger binding at younger ages than older ages. Interestingly, we found no significant difference in the expression levels of Hsc70-GFP, stv-GFP, and over-expression of $p38Kb^{KD}$ with age (Figure S1A-B, D) while levels of HspB8-GFP increased with age (Figure S1C). These data suggest that the age-dependent interaction between p38Kb and the CASA complex

may be due to changes in the physical interactions between these proteins rather than a reduction in protein levels.

To verify that endogenous p38Kb can interact with the CASA complex, we performed co-immunoprecipitations with muscle lysates from flies expressing either endogenously GFP tagged Hsc70-4, HspB8 or stv in a wild type background and probed for endogenous activated p38K that is dual phosphorylated on the TGY motif. We find that all three members of the CASA can co-immunoprecipitate with endogenous phosphorylated p38K in the muscle (Figure 2O). These results suggest that p38Kb is able to physically interact with the CASA complex.

p38Kb acts downstream of the CASA complex.

As p38Kb physically interacts with the CASA complex, we next tested if p38Kb is acting upstream activity of the complex to promote the initial recognition of misfolded proteins or the downstream activity of the complex to direct un-foldable proteins to the autophagosome. As BAG-3/stv provides both the specificity to the CASA complex and is involved in the handoff of damaged proteins to p62/ref(2)p for autosomal degradation [21–25], we tested for genetic interactions between p38Kb and *stv*. *stv* null mutants have impaired locomotor functions, muscle degeneration and early lethality [19,36]. Due to the severity of these null phenotypes, we utilized *stv* RNAi lines to generate an allelic series of *stv* loss of function in the muscle. We find that weak inhibition of stv (UAS-stv RNAi^{34408} MHC-GAL4) had no effect on protein aggregation (Table S6). However, moderate inhibition of stv (UAS-stv RNAi^{34409} MHC-GAL4) results in increased protein aggregate number and size (Figure 3A-B and Table S7) and results in a decrease in lifespan particularly in the first half of life as compared to outcrossed controls (Figure 3C and Table S8). Strong inhibition of *stv* (UAS-stv RNAi^{34408} Mef2-GAL4) leads to a severely reduced lifespan of ~4 days on average (Figure 3D and Table S9).

If p38Kb acts to regulate the downstream activity of the CASA complex, then over-expression of p38Kb should rescue these *stv* RNAi phenotypes. We find that over-expression of p38Kb rescues both protein aggregate number and size in the *stv* moderate inhibition background (Figure 3A-B and Table S7) and also rescues the lifespan defect (Figure 3C and Table S9). Furthermore, p38Kb over-expression is able to partially rescue the decreased lifespan exhibited by strong *stv* inhibition increasing average lifespan from 4 days to 13 days (Figure 3D and Table S10). To further test if p38Kb acts downstream of the CASA complex, we combined loss of p38Kb with CASA complex over-expression. If p38Kb acts downstream of the CASA complex, then over-expression of the CASA complex members in the p38Kb mutant background will not be able to rescue the p38Kb mutant phenotypes. We find that over-expression of stv in the p38Kb mutants not only fails to rescue the p38Kb mediated short lifespan defect but reduces the lifespan further (Figure 3E and Table S11). This is particularly striking as over-expression of stv in a wild type background does not significantly affect lifespan (Figure 4H and Table S12) as compared to the outcrossed transgene control (p value = 0.195). This suggests that p38Kb may be a limiting factor in regulating the downstream activity of the CASA complex in which it hands the poly-ubiquitinated misfolded proteins to ref(2)p for degradation through the autophagosome.

p38Kb regulates the activity of the CASA complex in protein homeostasis.

If p38Kb is a limiting factor for stv function, then the combined over-expression of p38Kb and stv may result in a further beneficial effect. We find that over-expression of stv alone results in fewer aggregates at young and old ages (Figure 4A-B and Table S13) and smaller aggregates with age (Figure 4D and Table S13) as compared to outcrossed controls. However, co-over-expression of p38Kb and stv does not result in a further reduction in aggregate number as compared to over-expression of p38Kb or stv

alone (Figure 4A and Table S13). By 5 weeks of age, co-over-expression of p38Kb and stv flies have comparable aggregate number to controls (Figure 4B and Table S13). Conversely, p38Kb and stv co-over-expression results in a reduction in aggregate size at a young age compared to over-expression of stv alone (Figure 4C and Table S13, p value < 0.001), suggesting that p38Kb is a limiting factor for stv function in regulating aggregate size. Unlike with aggregate number, the aggregates remain significantly smaller in size as the flies age in the combined over-expression background (Figure 4D and Table S13). We also find that co-over-expression of p38Kb and stv leads to an additional 5% increase in lifespan relative to p38Kb over-expression alone (Figure 4H and Table S12). Interestingly, the co-over-expression animals show a very similar lifespan to the p38Kb over-expression alone animals until ~day 50, when the p38Kb alone animals begin to die at a faster rate (Figure 4H). One explanation is that co-over-expression of p38Kb and stv provides beneficial effects in early adulthood that continue throughout adulthood leading to increased lifespan despite the presence of protein aggregates. Another possibility is that aggregate size is a reflection of aggregate content. If the CASA complex can only target a subset of proteins for refolding or degradation, then increasing CASA complex activity could lead to smaller aggregates as the CASA targets are effectively degraded through an interaction with p38Kb and ref(2)p rather than aggregating. Therefore, size and/or content may play a more important role in determining lifespan as compared to overall aggregate number.

p38Kb is required for proper localization of stv in the muscle.

Since we find that p38Kb acts between stv and ref(2)p in regulating protein aggregation, we hypothesize that p38Kb plays a role in stabilizing the transfer of misfolded proteins primed for degradation from the CASA complex to ref(2)p. If so, then over-expression of p38Kb would lead to increased efficiency in targeting misfolded

388 proteins to the autophagosome (Figure 1M-T), and inhibition of p38Kb would lead to an
389 increase in protein aggregation (Figure 1E-L). In addition, loss of p38Kb may lead to a
390 failure of stv to maintain its interaction with the CASA complex or to interact with ref(2)p.
391 Therefore, we tested if stv is still able to localize to the Z-disc in the absence of p38Kb.
392 We find that in p38Kb null mutants, stv is more diffuse throughout the muscle but is still
393 able to localize to the Z-disc and M-line in (Figure 4E-G), suggesting that its localization
394 is partially impaired in the absence of p38Kb. Furthermore, we find that the localization
395 of the CASA complex member HspB8 in the muscle is unaffected by loss of p38Kb
396 (Figure S2). These data indicate that p38Kb may play a role in stabilizing the interaction
397 between the CASA complex and stv that allows stv to direct misfolded proteins to
398 ref(2)p.
399
400 **Lamin protein binds to the CASA complex and accumulates in stv RNAi and**
401 **p38Kb mutants.**
402 In order to determine if p38Kb might be playing a role in the targeting of
403 misfolded proteins from stv to ref(2)p, we first needed to identify a protein target of both
404 stv and p38Kb. Therefore, we focused on proteins associated with Limb-Griddle
405 Muscular Dystrophy (LGMD), which is caused by mutations in either BAG-3 (stv) or
406 HspB8 [37–39]. In addition, p38K signaling has been implicated in LGMD [40–42]. *Drosophila*
407 have 19 orthologues of LGMD proteins, one of which is Lamin A/C (Lamin or Lamin Dm0
408 in flies). Lamin is of particular interest since mutations in Lamin A/C also result in the
409 accelerated aging disorder Hutchinson-Gilford progeria [43–45], and Lamin has been shown
410 to aggregate under oxidative stress conditions [46]. Mutations in Lamin A/C are also
411 sufficient to induce Lamin aggregation and abnormal nuclear morphology in human cell
412 culture, *C. elegans*, and *Drosophila* systems [44,47–54]. Furthermore in *Drosophila*, Lamin

413 knockouts have similar phenotypes to p38Kb and/or stv mutants, such as reduced
414 locomotor function and increased activity of the Nrf-2/Keap-1 pathway [49,55,56].

415 If Lamin is a target of the CASA complex, then decreased activity of the CASA
416 complex should result in an accumulation of Lamin protein. We find that Lamin levels do
417 not change with age (Figure 5A), however, inhibition of stv results in a significant
418 increase in the total amount of Lamin protein regardless of age (Figure 5A-B, p value
419 0.028). Interestingly, loss of p38Kb leads to an age-dependent increase in Lamin protein
420 as compared to age matched controls (Figure 5C-D, p value = 0.006643). As the
421 association between p38Kb and the CASA seems to decline with age (Figure 2L-N),
422 these data suggest that p38Kb activity later in life is important for maintaining protein
423 homeostasis and lifespan.

424 To investigate if Lamin is accumulating in the protein aggregates, we performed
425 fractionation experiments in which we find that Lamin is predominantly found in fractions
426 5-7 in controls with the majority concentrated in faction 6 (Figure 5E). Interestingly, we
427 also find a high molecular weight from of Lamin mainly restricted to fraction 5 (Figure
428 5E). In addition, we also observe that both the main and high molecular weight Lamin
429 species are in the aggregate containing pellet (Figure 5E). We next tested how loss of
430 p38Kb affects the aggregation of Lamin and find that p38Kb mutants have decreased
431 Lamin in fractions 5-7 with a concurrent increase of both the main and high molecular
432 weight species of Lamin in the pellet (Figure 5E). This suggests that Lamin is a target of
433 p38Kb and that loss of p38Kb results in increased aggregation of Lamin.

434

435 Of interest is this high molecular weight form of Lamin, which is present in
436 fraction 5 and the aggregates (Figure 5E). One important protein domain in Lamin is the
437 CaaX box, which is farnesylated and required for Lamin localization to the inner nuclear
438 membrane[57–60]. To test if this might be a farnesylated form of Lamin, we utilized the

439 Lam^{A25} mutant which has a frameshift that results in the loss of the C-terminal CaaX
440 box[61]. We find that the high molecular weight form of Lamin is lost in the Lam^{A25} mutant
441 whereas the predominant 75kDa band of Lamin is still present (Figure 5F). These data
442 suggest that the high molecular weight Lamin we observe is the farnesylated form.
443
444 In addition to farnesylation, Lamin can also be phosphorylated by a variety of
445 kinases that can change the solubility of Lamin [54,62]. For example, in a *Drosophila* cell
446 culture system, a phospho-mimic mutation at Ser45 (the equivalent of Ser22 in humans)
447 results in Lamin aggregation in both the nucleus and cytoplasm [54]. This serine residue is
448 phosphorylated by the cd2 kinase [63], but also happens to be a potential p38K
449 phosphorylation site. Therefore, we tested if the levels of phospho- Ser45 Lamin are
450 altered in p38Kb mutants. We find that phospho-Lamin levels are not significantly altered
451 in the p38Kb mutants (Figure 5G-H p=0.09), suggesting that p38Kb is not required for
452 Ser45 phosphorylation. We next examined if phosphorylated Lamin is also present in the
453 aggregates. We find that in controls, phosphorylated Lamin is present in factions 5-7
454 with low amounts in the pellet (Figure 5I). We also observe a low molecular weight
455 phospho-Lamin form that appears in the pellet (Figure 5I). In the p38Kb mutants,
456 phospho-Lamin expression is reduced in fractions 6 and 7 and accumulates in the pellet
457 (Figure 5I). Furthermore, increasingly smaller low molecular weight species of phospho-
458 Lamin are present in the p38Kb$^{\Delta 45}$ mutants including the pellet (Figure 5I), suggesting
459 that loss of p38Kb prevents the effective clearance of these Lamin cleavage forms.
460 Interestingly, loss of the Lamin CaaX box does not affect these lower molecular weight
461 forms, however, it does result in an increase in the phosphorylation of full-length Lamin
462 (Figure 5F). Additionally, we do not detect phosphorylation positive high molecular
463 weight forms of Lamin (Figure 5F), suggesting that farnesylated lamin is not
464 phosphorylated at Ser45. These data combined with our finding that full length Lamin is

phosphorylated, suggest that when Lamin is unphosphorylated it is prone to farnesylation that may lead to aggregation.

To determine if Lamin is a direct target of p38Kb and the CASA complex, we tested if Lamin can bind to the CASA complex. We immunoprecipitated endogenously GFP tagged HspB8, Hsc70-4 and stv from adult *Drosophila* muscle and probed for endogenous Lamin. We find that full-length Lamin co-immunoprecipitates with all three members of the CASA complex (Figure 6A), but do not detect binding with either the higher or lower molecular weight forms of Lamin found in the fractions (Figure 5E and I). Furthermore, we expressed either a nuclear localization signal tagged GFP or Lamin tagged with GFP in the muscle and found that endogenous stv co-immunoprecipitates with Lamin (Figure 6B). These data suggest that the CASA complex is able to bind to misfolded forms of full-length Lamin for targeting to the autophagosome.

As we hypothesize that p38Kb is interacting with the CASA complex at the point in which the misfolded targets are handed over to ref(2)p for degradation, we tested if p38Kb also binds to Lamin. We find that p38Kb^{KD} expressed in the muscle co-immunoprecipitates with both high and low molecular weight forms of Lamin (Figure 6C). Interestingly, p38Kb physically interacts with the aggregate prone low molecular weight species of Lamin as opposed to the predominant full-length form of Lamin (Figure 6C). More striking is that p38Kb^{KD} physically interacts with increasingly larger forms of Lamin (Figure 6C), suggesting that p38Kb is interacting with the poly-ubiquitinated forms of Lamin.

We have developed a model in which misfolded proteins are targeted by stv to the CASA complex. Those proteins that cannot be refolded are then tagged with poly-

ubiquitin. These poly-ubiquitinated proteins are handed off to ref(2)p in a process mediated by p38Kb. This model predicts that in p38Kb mutants these poly-ubiquitinated proteins accumulate and then form aggregates. It additionally predicts that over-expression of p38Kb would lead to increased efficiency of the poly-ubiquitinated proteins being targeted to the autophagosome. This model would also predict that misfolded full-length Lamin would bind to the CASA complex for refolding. If Lamin cannot be refolded it is then poly-ubiquitinated and transferred to ref(2)p through an interaction with p38Kb.

Discussion

We find that the aging gene p38Kb regulates age-dependent protein homeostasis through an interaction with the CASA complex and is acting at a step between the poly-ubiquitination of a un-foldable target and its transfer to ref(2)p for autolysosomal mediated degradation. Interestingly, we find that p38Kb is important for the proper localization of stv to the Z-disc but does not affect the localization of other complex members. This suggests that p38Kb may play a role in maintaining the interaction between stv and the CASA complex which may be necessary for target transfer to ref(2)p. stv has a conserved MAPK docking site as well several potential conserved p38K phosphorylation sites. Furthermore, mammalian p62 has been shown to bind to p38Kb in vitro through two domains [64], which are partially conserved in flies. Therefore, one possibility is that p38Kb mediated phosphorylation of stv facilitates the localization of a functional CASA complex to the Z-disc, where damaged proteins are rapidly turned over. Another possibility is that p38Kb binds to stv and ref(2)p and that the phosphorylation of stv is required for target hand-over to ref(2)p so that in the absence of p38Kb, stv cannot transfer targets to ref(2)p. A consequence of this may be that stv and the protein target together are released from the CASA complex, leading to mislocalization of stv. As we don't detect a decrease in phospho-Lamin in the p38Kb

517 mutants or find that the p38Kb can pull-down phospho-Lamin, it is unlikely that p38Kb is
518 directly phosphorylating the target proteins as a part of the stv-ref(2)p hand-over
519 process.
520
521 How protein aggregation contributes to aging and disease has been an area of
522 great interest. One outstanding question is if protein aggregation is a consequence or
523 cause of aging. It has been hypothesized that protein aggregates accumulate with age
524 as the amount of damaged or misfolded proteins increase. However, it is not clear
525 whether or not these aggregating proteins are toxic leading to tissue dysfunction and a
526 disease state. Previous studies have found that long-lived fly strains such as over-
527 expression of Foxo or parkin result in reduced protein aggregate formation [4,65].
528 Therefore, we hypothesized that decreased protein aggregation would lead to improved
529 measures of healthspan, while increased protein aggregation would lead to reduced
530 measures of healthspan. As expected, we find that the short-lived p38Kb mutants, which
531 exhibit premature locomotor behavior defects [16], have large and numerous protein
532 aggregates. Similarly, inhibition of stv results in increased aggregation and decreased
533 lifespan. We also find that over-expression of p38Kb leads to decreased protein
534 aggregation and increased lifespan. However, over-expression of stv leads to decreased
535 aggregate number but does not extend lifespan. One possibility is that decreasing
536 aggregation alone is not sufficient to promote lifespan extension. Another possibility is
537 that aggregate number is not as critical as aggregate size and/or content, particularly
538 early in life, for lifespan extension. We find that stv over-expression only results in
539 decreased aggregate size in older animals, however, co-over-expression of p38Kb and
540 stv leads to reduced aggregate size at a young and old ages and leads to a further
541 increase in lifespan. Thus, the turnover of specific toxic protein or subset of proteins
542 early in life may lead to a reduction in the exposure to these toxic species and a lifespan

543 extension. We find that Lamin, which is mutated to an aggregation prone protein form in
544 Hutchinson-Gilford progeria [44,53,62,66], is a target of p38Kb and the CASA complex.
545 Interestingly, p38Kb and Lamin mutants share similar phenotypes such as age-
546 dependent locomotor impairments [16,55,56] and upregulation of the Nrf-2/Keap-1 pathway
547 [16,49]. As loss of p38Kb leads to an accumulation of Lamin in the aggregates, this may be
548 toxic to the cell, leading to impaired locomotor function, increased stress and decreased
549 lifespan. Thus, we have found that one aging gene (p38Kb) regulates a second,
550 unrelated aging gene (Lamin) via the CASA complex. These data suggest a new link
551 between aging pathways and how they may converge through the regulation of protein
552 homeostasis.
553

554 **Acknowledgements**

555 We would also like to acknowledge the Bloomington Drosophila Stock Center (NIH
556 P40OD018537), the Vienna Drosophila Resource Center, and Kyoto Stock Center for
557 providing fly stocks used in this study. A. Vrailas-Mortimer was funded by start-up funds
558 from the University of Denver, a Knoebel Center for the Study of Aging pilot grant, start-
559 up funds from Illinois State University and was supported by the National Institute of
560 Arthritis and Musculoskeletal and Skin Diseases of the National Institutes of Health
561 under Award Number R15AR070505. The content is solely the responsibility of the
562 authors and does not necessarily represent the official views of the National Institutes of
563 Health. S. Sanyal was funded by startup funds from Emory University. S. Ryan was
564 supported by a Knoebel Center for the Study of Aging pilot grant to A. Vrailas-Mortimer
565 and S. Barbee, N. Mortimer was funded by start-up funds from Illinois State University.
566 The funders had no role in study design, data collection and analysis, decision to
567 publish, or preparation of the manuscript.
568

Figure Legends

Fig 1. p38Kb regulates age-dependent protein homeostasis.

Confocal micrographs of polyubiquitin positive protein aggregates in the adult indirect flight muscle in **A)** a precise excision genetic background control p38Kb$^{Ex41/\ Ex41}$ and **B)** p38Kb $^{\Delta 45/\Delta 45}$ null mutants at three weeks of age and in **C)** outcrossed Mef2-GAL4 controls (Mef2>w^{11118}) and **D)** UAS-p38Kb^{wt} Mef2-GAL4 (Mef2>p38Kb^{wt}) over-expression animals at 5 weeks of age. Scale bar equals 6.2 μm. Box-Whisker plots of aggregate number in p38Kb $^{\Delta 45/\Delta 45}$ mutants as compared to p38Kb$^{Ex41/Ex41}$ controls at **E)** 1 week and **F)** 3 weeks of age and aggregate size at **G)** 1 week and **H)** 3 weeks of age. Aggregate number in p38Kb^{KD} Mef2-GAL4 (Mef2>p38Kb^{KD}) and outcrossed Mef2-GAL4 controls at **I)** 1 week and **J)** 5 weeks of age and aggregate size at **K)** 1 week and **L)** 5 weeks of age. Aggregate number in strong p38Kb over-expression animals and outcrossed Mef2-GAL4 controls at **M)** 1 week and **N)** 5 weeks of age and aggregate size at **O)** 1 week and **P)** 5 weeks of age. Aggregate number in moderate p38Kb over-expression (MHC>p38Kb^{wt}) animals and outcrossed MHC-GAL4 controls (MHC>w^{1118}) at **Q)** 1 week and **R)** 5 weeks of age and aggregate size at **S)** 1 week and **T)** 5 weeks of age.

Fig 2. p38Kb regulates aging phenotypes through ref(2)p.

A-C) A subset of polyubiquitinated protein aggregates (green) in 3 week old p38Kb$^{Ex4/Ex41}$ control muscle contain K63 ubiquitinated (magenta) proteins (white arrows). **D-E)** Protein aggregate number in ref(2)p heterozygous mutant backgrounds at **D)** 1 week and **E)** 5 weeks. Loss of a single copy of ref(2)p prevents the p38Kb mediated reduced protein aggregation at 1 week and 5 weeks of age. Asterisks denote a p-value of ≤0.001. **(F-I)** Localization of a FLAG-tagged p38Kb (green in **F-I** and **F''-I''**) in the

595 adult indirect flight muscle. **F)** FLAG-tagged p38Kb localizes to the Z-disc (arrows) as
596 exhibited by colocalization with the Z-disc protein alpha-actinin (magenta, **F'** and **F''**), as
597 well as the M-line (arrowheads). **G-I)** p38Kb colocalizes with each CASA complex
598 member (magenta, **G'-I'**) at the Z-disc. Over-expression of a FLAG tagged p38Kb in the
599 muscle in **G**) an endogenous Hsc70-GFP fusion protein background, **H**) an endogenous
600 HspB8-GFP fusion protein background, and **I)** a wildtype background with endogenous
601 levels of stv. **J-K)** Muscle lysates expressing control and Mef2-GAL4 UAS-p38Kb$^{KD\text{-}FLAG}$
602 in either **J)** an endogenously expressed HspB8-GFP background or **K)** a wildtype
603 background were immunoprecipitated using anti-FLAG coated beads. **J)** Immunoblots
604 were probed with anti-GFP to detect the presence of HspB8 in the IP lysates or with **K)**
605 anti-stv to detect the presence of stv in the IP lysates. **L-N)** Muscle lysates expressing
606 p38Kb $^{KD\text{-}FLAG}$ in an endogenously expressed **L)** Hsc70-GFP, **M)** HspB8-GFP and **N)** stv-
607 GFP background were immunoprecipitated using anti-GFP coated beads. Immunoblots
608 were probed with anti-FLAG to detect the presence of p38Kb in the IP lysates. Note: stv
609 is tagged with both GFP and FLAG. **O)** Endogenous phospho-p38 co-
610 immunoprecipitates with Hsc70-4-GFP, HspB8-GFP, and stv-GFP. Muscle lysates were
611 immunoprecipitated with anti-GFP beads, and immunoblots were probed with anti-
612 phospho-p38K.
613
614 **Fig 3. p38Kb genetically interacts with stv to regulate protein homeostasis and**
615 **lifespan. A)** Protein aggregate number and **B)** size in the moderate stv knockdown
616 background using MHC-GAL4 at 5 weeks. Asterisks denote a p-value of ≤0.001. **C)**
617 Moderate over-expression of p38Kb (red line) results in an increased lifespan as
618 compared to the MHC-GAL4 controls and p38Kb transgene control (black line and gray
619 lines, respectively). Moderate knockdown of stv using the MHC-GAL4 results in a
620 decreased lifespan (pink line compared to yellow and black lines) and is rescued by

p38Kb over-expression (compare pink line to blue line). **D)** Strong over-expression of p38Kb (red line) results in an increased lifespan as compared to the Mef2-GAL4 controls and p38Kb transgene control (black line and gray lines, respectively). Strong knockdown of stv using the Mef2-GAL4 results in a decreased lifespan (pink line compared to yellow and black lines) and is partially rescued by p38Kb over-expression (compare pink line to blue line). **E)** Over-expression of stv in the p38Kb mutant background results in a further reduction of lifespan as compared to p38Kb mutant controls (compare blue line to red and grey lines).

Fig 4. p38Kb is limiting for stv function and localization.

Protein aggregate number at **A)** 1 week and **B)** 5 weeks and protein aggregate size at **C)** 1 week and **D)** 5 weeks measured in stv over-expression backgrounds. Over-expression of stv leads to reduced aggregate number at 1 and 5 weeks and aggregate size at 5 weeks. Co-over-expression of stv and p38Kb does not result in a further decrease in protein aggregate number but trends towards decreased aggregate size at both 1 and 5 weeks of age. Asterisks denote a p-value of ≤0.001 when compared to the GAL4 control. **E)** stv localizes to the adult muscle Z-disc and M-line (white arrows) in control animals. **F)** stv localization is disrupted in p38Kb mutants. **G)** Quantification of average pixel density. **H)** Over-expression of stv alone has no significant effect on lifespan (pink line as compared to yellow and black lines), however, co-over-expression of stv and p38Kb results in a further increase in lifespan (compare red line to blue line).

Fig 5. p38Kb and stv regulate Lamin aggregation.

A) Immunoblot analysis of stv-RNAi and GAL4 controls flies muscle lysates probed with anti-Lamin and **B)** quantified using densitometry. **C)** Immunoblot analysis of

p38Kb$^{Ex41/Ex41}$ control and p38Kb $^{\Delta45/\Delta45}$ mutant muscle lysates probed with anti-Lamin and **D)** quantified using densitometry. **H)** Immunoblots of sucrose gradient fractions from 3 week old p38Kb$^{Ex41/Ex41}$ control and p38Kb $^{\Delta45/\Delta45}$ mutant muscle probed with anti-Lamin. **G)** Immunoblot analysis of p38Kb$^{Ex41/Ex41}$ control and p38Kb $^{\Delta45/\Delta45}$ mutant muscle lysates probed with anti-phospho Lamin and **H)** quantified using densitometry. **I)** Immunoblots of sucrose gradient fractions from 3 week old p38Kb$^{Ex41/Ex41}$ control and p38Kb $^{\Delta45/\Delta45}$ mutant muscle probed with anti-phospho-Lamin.

Fig 6. p38Kb and stv physically interact with Lamin.

A) Endogenous HspB8-GFP, Hsc70-GFP and stv-GFP-FLAG fusion proteins were immunoprecipitated from adult muscle lysate using anti-GFP coated beads. Immunoblots were probed with anti-Lamin and anti-GFP. **B)** A nls-GFP or Lamin-GFP was expressed in muscles using MHC-GAL4. GFP proteins were immunoprecipitated from adult muscle lysates using anti-GFP coated beads. Immunoblots were probed with anti-stv and anti-GFP. C) p38Kb^{KD} was expressed in muscles using Mef2-GAL4. p38Kb was immunoprecipitated from adult muscle lysates using anti-FLAG coated beads. Immunoblots were probed with anti-lamin and anti-FLAG.

Fig S1. CASA complex expression with age. Immunoblot analysis of **A)** endogenously GFP tagged Hsc70-4, **B)** endogenously GFP tagged HspB8, **C)** stv, and **D)** the FLAG tagged p38Kb kinase dead transgene with age. Asterisks denote a p value of ≤0.05 as compared to the 3 day time point.

Fig S2. Localization of HspB8 in p38Kb mutants. Endogenously GFP-tagged HspB8 was analyzed in the muscle of three week old **A)** controls and **B)** p38Kb mutants. HspB8

672 (green) localizes to the Z-disc and M-line of the indirect flight muscle (actin in magenta)
673 in both control and p38Kb mutant animals.
674
675
676 **References**

677 1. Taylor, R. C. & Dillin, A. Aging as an event of proteostasis collapse. *Cold Spring*
678 *Harb. Perspect. Biol.* **3**, (2011).
679 2. Ben-Zvi, A., Miller, E. A. & Morimoto, R. I. Collapse of proteostasis represents an
680 early molecular event in Caenorhabditis elegans aging. *Proc. Natl. Acad. Sci. U. S.*
681 *A.* **106**, 14914–14919 (2009).
682 3. Cohen, E., Bieschke, J., Perciavalle, R. M., Kelly, J. W. & Dillin, A. Opposing
683 activities protect against age-onset proteotoxicity. *Science* **313**, 1604–1610 (2006).
684 4. Demontis, F. & Perrimon, N. FOXO/4E-BP signaling in Drosophila muscles regulates
685 organism-wide proteostasis during aging. *Cell* **143**, 813–825 (2010).
686 5. Morley, J. F., Brignull, H. R., Weyers, J. J. & Morimoto, R. I. The threshold for
687 polyglutamine-expansion protein aggregation and cellular toxicity is dynamic and
688 influenced by aging in Caenorhabditis elegans. *Proc. Natl. Acad. Sci. U. S. A.* **99**,
689 10417–10422 (2002).
690 6. Palazzolo, I. *et al.* Overexpression of IGF-1 in muscle attenuates disease in a mouse
691 model of spinal and bulbar muscular atrophy. *Neuron* **63**, 316–328 (2009).
692 7. Schnöder, L. *et al.* Deficiency of Neuronal p38α MAPK Attenuates Amyloid
693 Pathology in Alzheimer Disease Mouse and Cell Models through Facilitating
694 Lysosomal Degradation of BACE1. *J. Biol. Chem.* **291**, 2067–2079 (2016).
695 8. Webber, J. L. & Tooze, S. A. New insights into the function of Atg9. *FEBS Lett.* **584**,
696 1319–1326 (2010).

9. Liu, B., Cheng, Y., Zhang, B., Bian, H. & Bao, J. Polygonatum cyrtonema lectin induces apoptosis and autophagy in human melanoma A375 cells through a mitochondria-mediated ROS-p38-p53 pathway. *Cancer Lett.* **275**, 54–60 (2009).
10. Younce, C. W. & Kolattukudy, P. E. MCP-1 causes cardiomyoblast death via autophagy resulting from ER stress caused by oxidative stress generated by inducing a novel zinc-finger protein, MCPIP. *Biochem. J.* **426**, 43–53 (2010).
11. Duan, W.-J. *et al.* Silibinin activated p53 and induced autophagic death in human fibrosarcoma HT1080 cells via reactive oxygen species-p38 and c-Jun N-terminal kinase pathways. *Biol. Pharm. Bull.* **34**, 47–53 (2011).
12. Zhuang, Y., Li, Y., Li, X., Xie, Q. & Wu, M. Atg7 Knockdown Augments Concanavalin A-Induced Acute Hepatitis through an ROS-Mediated p38/MAPK Pathway. *PloS One* **11**, e0149754 (2016).
13. Henson, S. M. *et al.* p38 signaling inhibits mTORC1-independent autophagy in senescent human $CD8^+$ T cells. *J. Clin. Invest.* **124**, 4004–4016 (2014).
14. Luo, Y. *et al.* Autophagy regulates ROS-induced cellular senescence via p21 in a p38 MAPKα dependent manner. *Exp. Gerontol.* **46**, 860–867 (2011).
15. Rudolf, E., Rezáčová, K. & Cervinka, M. Activation of p38 and changes in mitochondria accompany autophagy to premature senescence-like phenotype switch upon chronic exposure to selenite in colon fibroblasts. *Toxicol. Lett.* **231**, 29–37 (2014).
16. Vrailas-Mortimer, A. *et al.* A muscle-specific p38 MAPK/Mef2/MnSOD pathway regulates stress, motor function, and life span in Drosophila. *Dev. Cell* **21**, 783–795 (2011).
17. Belozerov, V. E., Ratkovic, S., McNeill, H., Hilliker, A. J. & McDermott, J. C. In vivo interaction proteomics reveal a novel p38 mitogen-activated protein kinase/Rack1

722 pathway regulating proteostasis in Drosophila muscle. *Mol. Cell. Biol.* **34**, 474–484
723 (2014).
724 18. Guruharsha, K. G. *et al.* A protein complex network of Drosophila melanogaster. *Cell*
725 **147**, 690–703 (2011).
726 19. Arndt, V. *et al.* Chaperone-assisted selective autophagy is essential for muscle
727 maintenance. *Curr. Biol. CB* **20**, 143–148 (2010).
728 20. Stürner, E. & Behl, C. The Role of the Multifunctional BAG3 Protein in Cellular
729 Protein Quality Control and in Disease. *Front. Mol. Neurosci.* **10**, 177 (2017).
730 21. Behl, C. BAG3 and friends: co-chaperones in selective autophagy during aging and
731 disease. *Autophagy* **7**, 795–798 (2011).
732 22. Gamerdinger, M. *et al.* Protein quality control during aging involves recruitment of
733 the macroautophagy pathway by BAG3. *EMBO J.* **28**, 889–901 (2009).
734 23. Kettern, N., Dreiseidler, M., Tawo, R. & Höhfeld, J. Chaperone-assisted degradation:
735 multiple paths to destruction. *Biol. Chem.* **391**, 481–489 (2010).
736 24. Min, J.-N. *et al.* CHIP deficiency decreases longevity, with accelerated aging
737 phenotypes accompanied by altered protein quality control. *Mol. Cell. Biol.* **28**, 4018–
738 4025 (2008).
739 25. Terman, A., Gustafsson, B. & Brunk, U. T. Autophagy, organelles and ageing. *J.*
740 *Pathol.* **211**, 134–143 (2007).
741 26. Dietzl, G. *et al.* A genome-wide transgenic RNAi library for conditional gene
742 inactivation in Drosophila. *Nature* **448**, 151–156 (2007).
743 27. R. C. Team. R Foundation for Statistical Computing. (2015).
744 28. Lim, K. L. *et al.* Parkin mediates nonclassical, proteasomal-independent
745 ubiquitination of synphilin-1: implications for Lewy body formation. *J. Neurosci. Off.*
746 *J. Soc. Neurosci.* **25**, 2002–2009 (2005).

747 29. Olzmann, J. A. *et al.* Parkin-mediated K63-linked polyubiquitination targets misfolded
748 DJ-1 to aggresomes via binding to HDAC6. *J. Cell Biol.* **178**, 1025–1038 (2007).
749 30. Yung, C., Sha, D., Li, L. & Chin, L.-S. Parkin Protects Against Misfolded SOD1
750 Toxicity by Promoting Its Aggresome Formation and Autophagic Clearance. *Mol.*
751 *Neurobiol.* **53**, 6270–6287 (2016).
752 31. Hao, R. *et al.* Proteasomes activate aggresome disassembly and clearance by
753 producing unanchored ubiquitin chains. *Mol. Cell* **51**, 819–828 (2013).
754 32. Tan, J. M. M. *et al.* Lysine 63-linked ubiquitination promotes the formation and
755 autophagic clearance of protein inclusions associated with neurodegenerative
756 diseases. *Hum. Mol. Genet.* **17**, 431–439 (2008).
757 33. Katsuragi, Y., Ichimura, Y. & Komatsu, M. p62/SQSTM1 functions as a signaling hub
758 and an autophagy adaptor. *FEBS J.* **282**, 4672–4678 (2015).
759 34. Ulbricht, A. *et al.* Cellular mechanotransduction relies on tension-induced and
760 chaperone-assisted autophagy. *Curr. Biol. CB* **23**, 430–435 (2013).
761 35. Hattori, A., Mizuno, T., Akamatsu, M., Hisamoto, N. & Matsumoto, K. The
762 Caenorhabditis elegans JNK Signaling Pathway Activates Expression of Stress
763 Response Genes by Derepressing the Fos/HDAC Repressor Complex. *PLOS*
764 *Genet.* **9**, e1003315 (2013).
765 36. Coulson, M., Robert, S. & Saint, R. Drosophila starvin encodes a tissue-specific
766 BAG-domain protein required for larval food uptake. *Genetics* **171**, 1799–1812
767 (2005).
768 37. Sato, T. *et al.* DNAJB6 myopathy in an Asian cohort and cytoplasmic/nuclear
769 inclusions. *Neuromuscul. Disord. NMD* **23**, 269–276 (2013).
770 38. Selcen, D. *et al.* Mutation in BAG3 causes severe dominant childhood muscular
771 dystrophy. *Ann. Neurol.* **65**, 83–89 (2009).

772 39. Sarparanta, J. *et al.* Mutations affecting the cytoplasmic functions of the co-
773 chaperone DNAJB6 cause limb-girdle muscular dystrophy. *Nat. Genet.* **44**, 450–455,
774 S1-2 (2012).
775 40. Fanzani, A. *et al.* Hypertrophy and atrophy inversely regulate Caveolin-3 expression
776 in myoblasts. *Biochem. Biophys. Res. Commun.* **357**, 314–318 (2007).
777 41. Capanni, C. *et al.* Dysferlin in a hyperCKaemic patient with caveolin 3 mutation and
778 in C2C12 cells after p38 MAP kinase inhibition. *Exp. Mol. Med.* **35**, 538–544 (2003).
779 42. Suzuki, N. *et al.* Continuous administration of poloxamer 188 reduces overload-
780 induced muscular atrophy in dysferlin-deficient SJL mice. *Neurosci. Res.* **72**, 181–
781 186 (2012).
782 43. De Sandre-Giovannoli, A. *et al.* Lamin a truncation in Hutchinson-Gilford progeria.
783 *Science* **300**, 2055 (2003).
784 44. Eriksson, M. *et al.* Recurrent de novo point mutations in lamin A cause Hutchinson-
785 Gilford progeria syndrome. *Nature* **423**, 293–298 (2003).
786 45. Mounkes, L. C., Kozlov, S., Hernandez, L., Sullivan, T. & Stewart, C. L. A progeroid
787 syndrome in mice is caused by defects in A-type lamins. *Nature* **423**, 298–301
788 (2003).
789 46. Singla, A. *et al.* Lamin aggregation is an early sensor of porphyria-induced liver
790 injury. *J. Cell Sci.* **126**, 3105–3112 (2013).
791 47. Bank, E. M. *et al.* A laminopathic mutation disrupting lamin filament assembly
792 causes disease-like phenotypes in Caenorhabditis elegans. *Mol. Biol. Cell* **22**, 2716–
793 2728 (2011).
794 48. Casasola, A. *et al.* Prelamin A processing, accumulation and distribution in normal
795 cells and laminopathy disorders. *Nucleus* **7**, 84–102 (2016).
796 49. Dialynas, G. *et al.* Myopathic Lamin Mutations Cause Reductive Stress and Activate
797 the Nrf2/Keap-1 Pathway. *PLOS Genet.* **11**, e1005231 (2015).

798 50. Hübner, S., Eam, J. E., Hübner, A. & Jans, D. A. Laminopathy-inducing lamin A
799 mutants can induce redistribution of lamin binding proteins into nuclear aggregates.
800 *Exp. Cell Res.* **312**, 171–183 (2006).
801 51. Hübner, S., Eam, J. E., Wagstaff, K. M. & Jans, D. A. Quantitative analysis of
802 localization and nuclear aggregate formation induced by GFP-lamin A mutant
803 proteins in living HeLa cells. *J. Cell. Biochem.* **98**, 810–826 (2006).
804 52. Ahmed, M. S., Ikram, S., Bibi, N. & Mir, A. Hutchinson-Gilford Progeria Syndrome: A
805 Premature Aging Disease. *Mol. Neurobiol.* **55**, 4417–4427 (2018).
806 53. Barascu, A. *et al.* Oxidative stress induces an ATM-independent senescence
807 pathway through p38 MAPK-mediated lamin B1 accumulation. *EMBO J.* **31**, 1080–
808 1094 (2012).
809 54. Zaremba-Czogalla, M. *et al.* The Different Function of Single Phosphorylation Sites
810 of Drosophila melanogaster Lamin Dm and Lamin C. *PLoS ONE* **7**, (2012).
811 55. Li, Y. *et al.* Lamin Mutations Accelerate Aging via Defective Export of Mitochondrial
812 mRNAs through Nuclear Envelope Budding. *Curr. Biol. CB* **26**, 2052–2059 (2016).
813 56. Muñoz-Alarcón, A. *et al.* Characterization of lamin Mutation Phenotypes in
814 Drosophila and Comparison to Human Laminopathies. *PLOS ONE* **2**, e532 (2007).
815 57. Kitten, G. T. & Nigg, E. A. The CaaX motif is required for isoprenylation, carboxyl
816 methylation, and nuclear membrane association of lamin B2. *J. Cell Biol.* **113**, 13–23
817 (1991).
818 58. Holtz, D., Tanaka, R. A., Hartwig, J. & McKeon, F. The CaaX motif of lamin A
819 functions in conjunction with the nuclear localization signal to target assembly to the
820 nuclear envelope. *Cell* **59**, 969–977 (1989).
821 59. Meshorer, E. & Gruenbaum, Y. Gone with the Wnt/Notch: stem cells in
822 laminopathies, progeria, and aging. *J. Cell Biol.* **181**, 9–13 (2008).

823 60. Polychronidou, M., Hellwig, A. & Grosshans, J. Farnesylated nuclear proteins
824 Kugelkern and lamin Dm0 affect nuclear morphology by directly interacting with the
825 nuclear membrane. *Mol. Biol. Cell* **21**, 3409–3420 (2010).
826 61. Patterson, K. *et al.* The functions of Klarsicht and nuclear lamin in developmentally
827 regulated nuclear migrations of photoreceptor cells in the Drosophila eye. *Mol. Biol.*
828 *Cell* **15**, 600–610 (2004).
829 62. Cao, K., Capell, B. C., Erdos, M. R., Djabali, K. & Collins, F. S. A lamin A protein
830 isoform overexpressed in Hutchinson-Gilford progeria syndrome interferes with
831 mitosis in progeria and normal cells. *Proc. Natl. Acad. Sci. U. S. A.* **104**, 4949–4954
832 (2007).
833 63. Machowska, M., Piekarowicz, K. & Rzepecki, R. Regulation of lamin properties and
834 functions: does phosphorylation do it all? *Open Biol.* **5**, (2015).
835 64. Saito, A., Kawai, K., Takayama, H., Sudo, T. & Osada, H. Improvement of
836 photoaffinity SPR imaging platform and determination of the binding site of
837 p62/SQSTM1 to p38 MAP kinase. *Chem. Asian J.* **3**, 1607–1612 (2008).
838 65. Rana, A., Rera, M. & Walker, D. W. Parkin overexpression during aging reduces
839 proteotoxicity, alters mitochondrial dynamics, and extends lifespan. *Proc. Natl. Acad.*
840 *Sci. U. S. A.* **110**, 8638–8643 (2013).
841 66. Burke, B. & Stewart, C. L. The nuclear lamins: flexibility in function. *Nat. Rev. Mol.*
842 *Cell Biol.* **14**, 13–24 (2013).
843

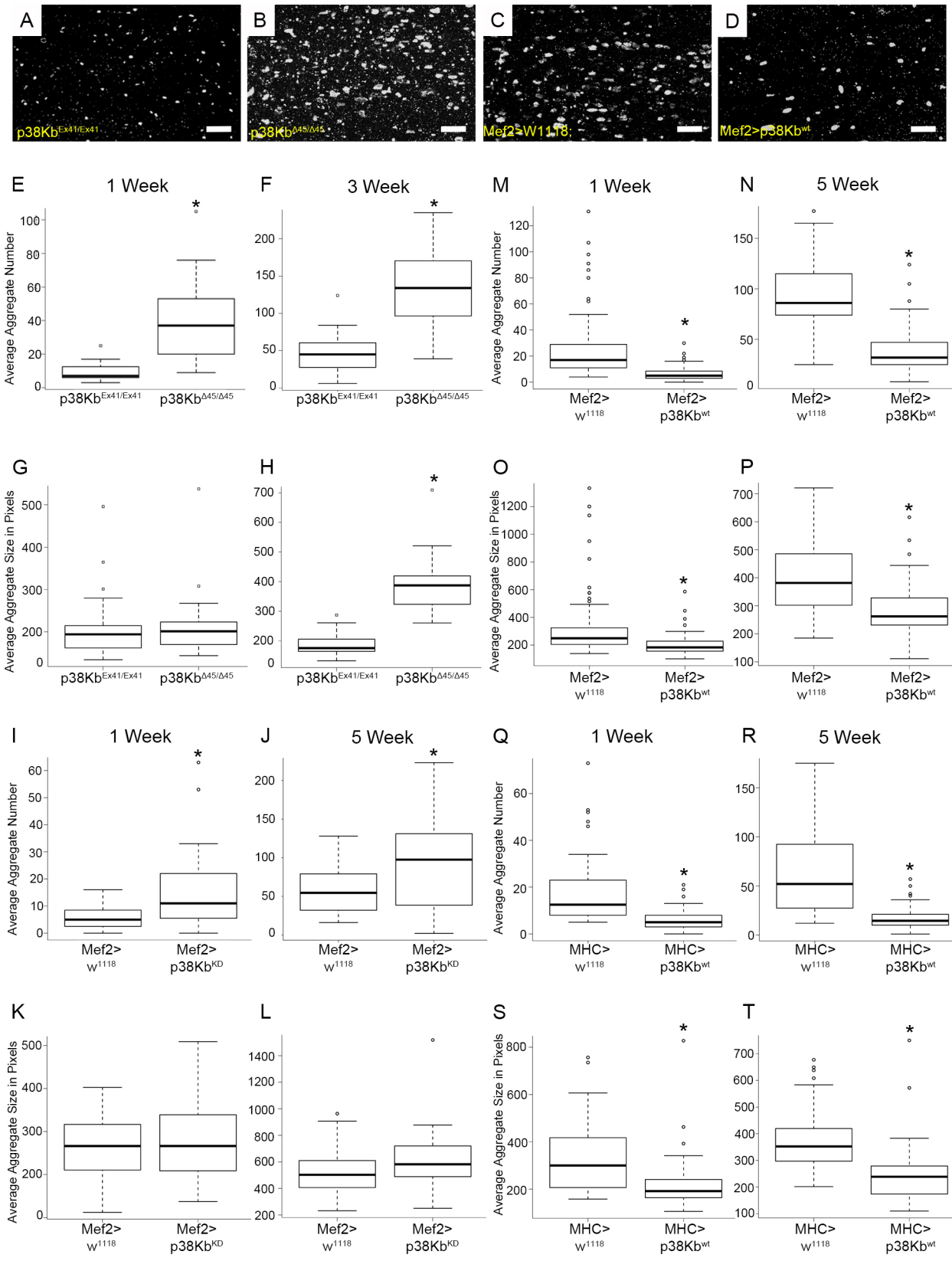

Figure 1

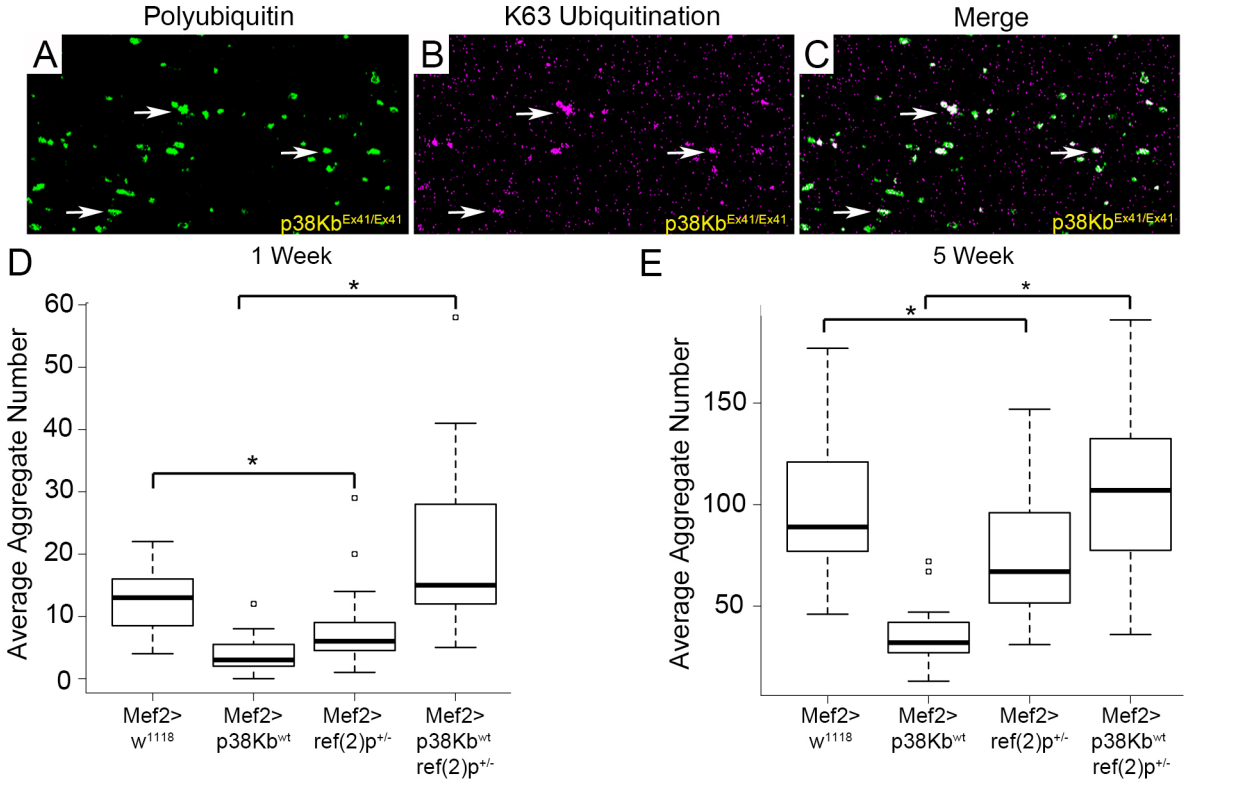

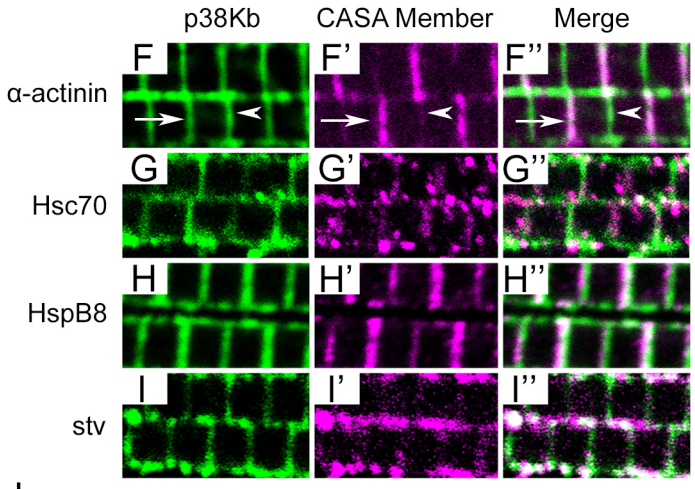

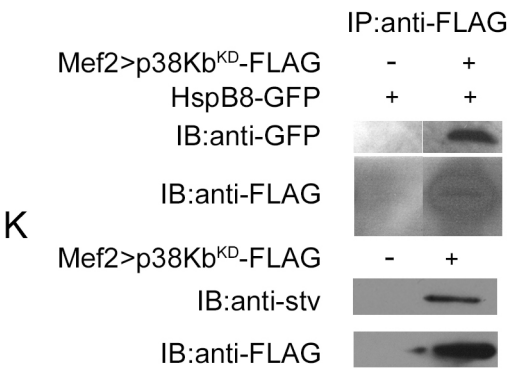

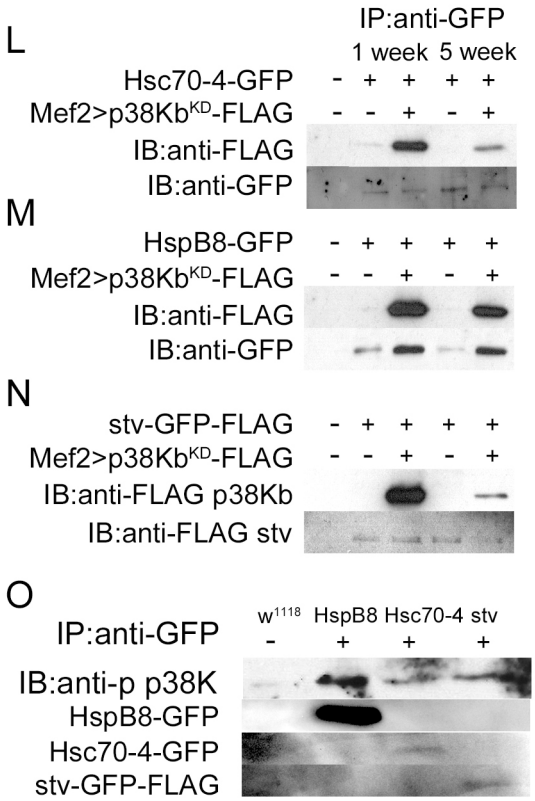

Figure 2

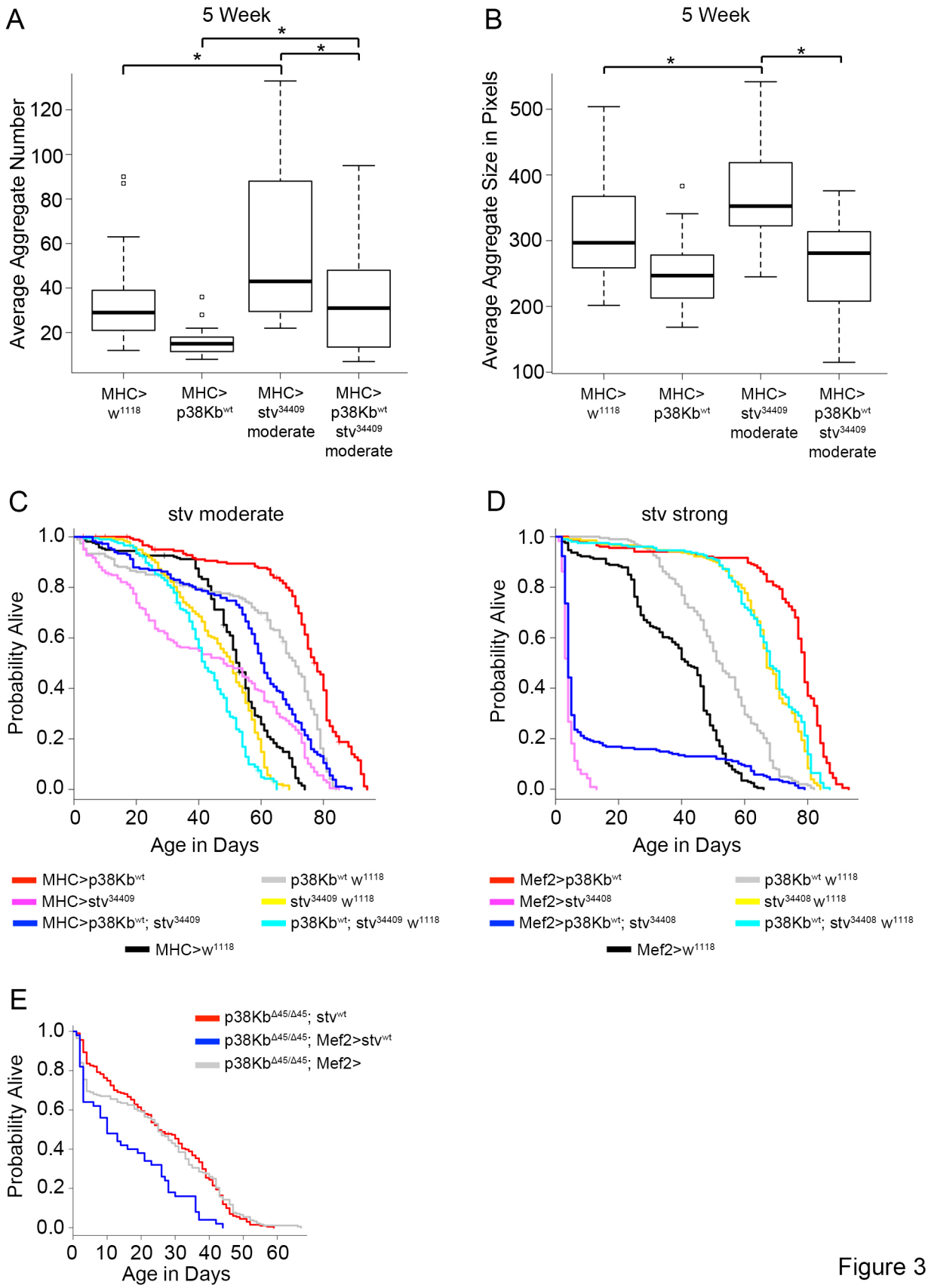

Figure 3

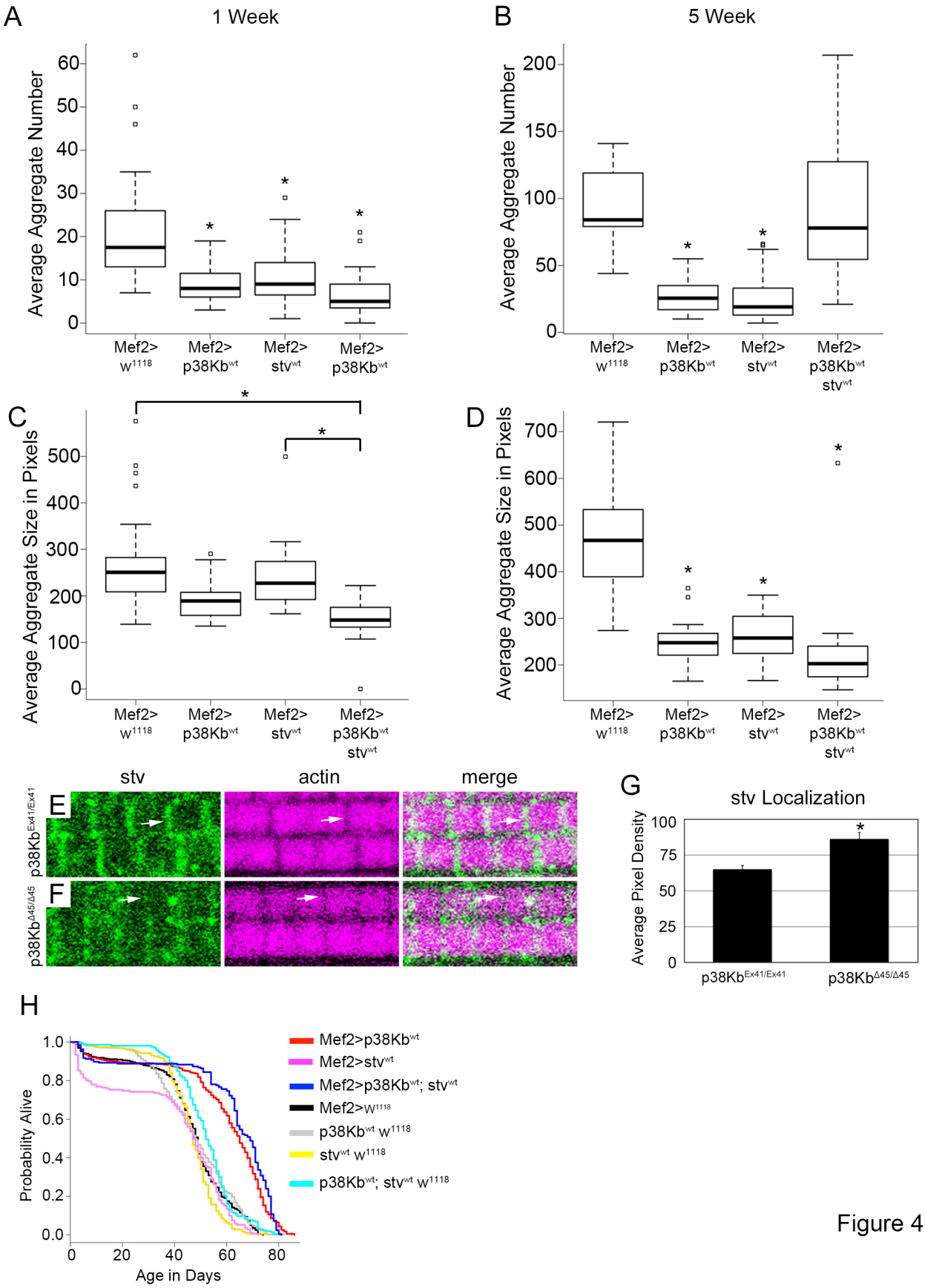

Figure 4

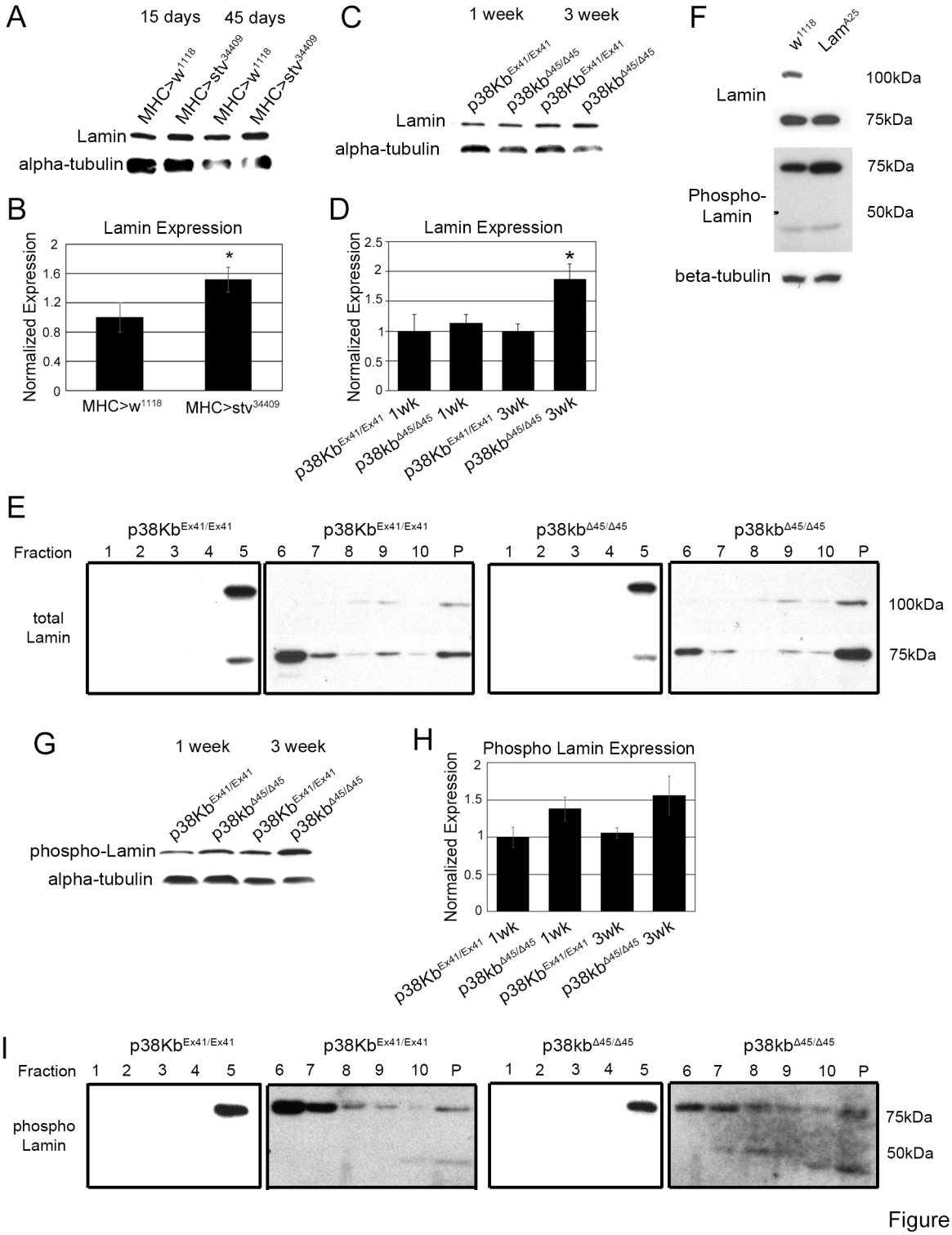

Figure 5

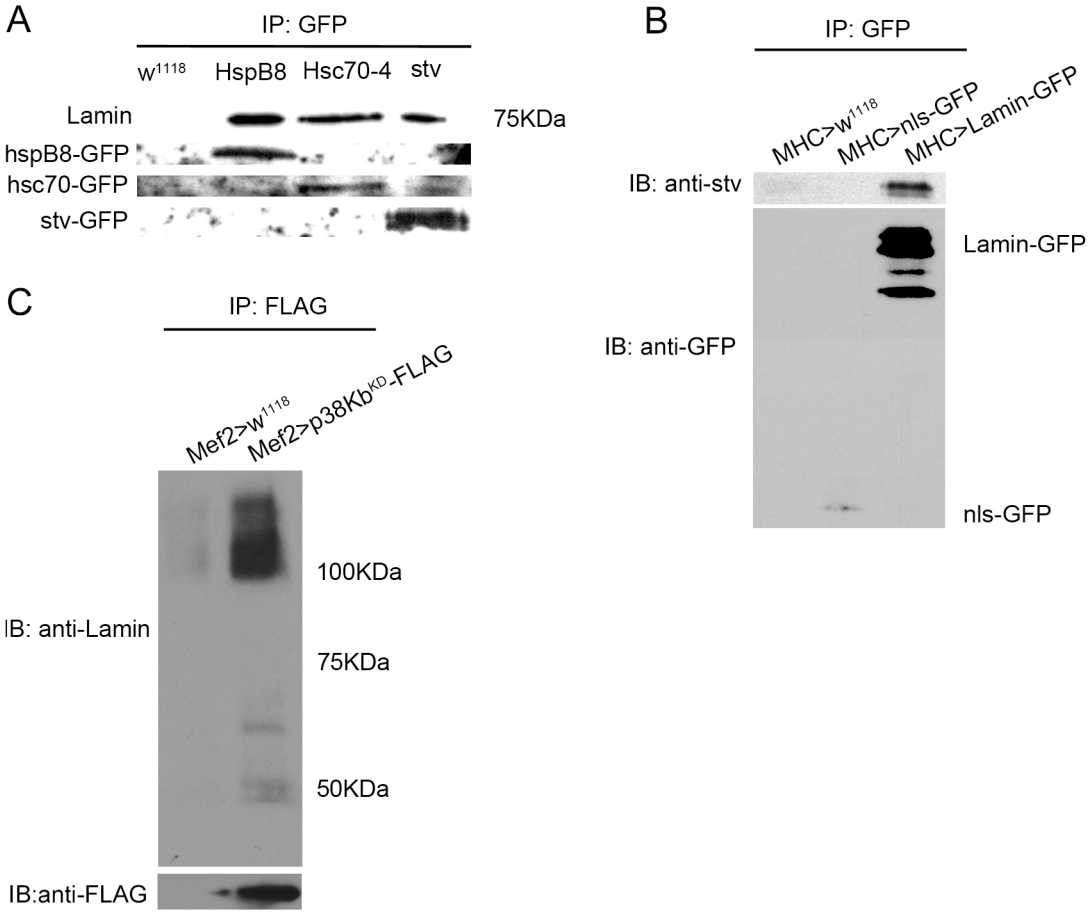

Figure 6